Available online at www.sciencedirect.com
ScienceDirect
Tetrahedron Letters 49 (2008) 2311–2315
Tetrahedron Letters

A cationic porphyrin-based self-assembled film for mercury ion detection

Zhen Fang, Bin Liu *

Department of Chemical and Biomolecular Engineering, 4 Engineering Drive 4, National University of Singapore, Singapore 117576, Singapore

Received 23 November 2007; revised 14 January 2008; accepted 31 January 2008
Available online 7 February 2008

Abstract

A cationic 5,15-(*p*-(9,9-bis(6-trimethylammoniumhexyl)fluorenylethynyl)phenyl)porphyrin tetrabromide was synthesized and the self-assembled films were used for Hg^{2+} detection in aqueous media. The detection response is based on fluorescence quenching of the porphyrin molecule upon coordination with Hg^{2+}. The detection shows high selectivity for Hg^{2+} over Cu^{2+}, Zn^{2+}, Pb^{2+}, Cd^{2+}, Mn^{2+}, Ni^{2+}, Co^{2+} and Ca^{2+}. A linear response toward Hg^{2+} in a concentration range of 1×10^{-10}–1×10^{-6} M was observed for the film with a detection limit of 0.1 nM. The cationic porphyrin film shows higher stability and significant improvement in detection sensitivity, as compared to other porphyrin-based sensors. The amphiphilic cationic nature of the porphyrin synthesized also allows for the direct deposition of a porphyrin layer on a bare glass surface through self-assembly.

Keywords: Cationic porphyrin; Fluorene; Fluorescence quenching; Mercury; Self-assembly

There has been growing interest in using porphyrins as active materials for analytical applications owing to their large absorption coefficient and well tunable fluorescence emission.[1] In addition, porphyrins show high sensitivity to metal ions, and display photometric changes in the region of the Soret band (~400 nm, $S_0 \rightarrow S_2$) as well as the minor Q bands (500–700 nm, $S_0 \rightarrow S_1$) upon metal ion chelation.[2] Large Stoke's shifts (>200 nm) are observed for most porphyrins because of the fast vibration relaxation from $S_2 \rightarrow S_1$, while the maximum emission is located in the Q-bands and can be attributed to $S_1 \rightarrow S_0$ transitions. Prominent fluorescence quenching occurs once metalloporphyrins are formed.[3] This property has been widely used for sensing heavy metal ions in aqueous solutions.[4–8]

Both neutral and charged porphyrins have been used for the detection of mercury ions in aqueous media. A lyophilized 5,10,15,20-tetraphenylporphyrin (H_2tpp) embedded in a polyvinyl chloride (PVC) membrane was operated through ion exchange between hydrogen and mercury(II) in aqueous solutions, which showed a detection limit (DL) of 4.0×10^{-8} M.[4] By incorporating alkylated β-cyclodextrin (β-CD) in the H_2tpp solution, significant fluorescence enhancement (up to 45-fold) was observed, which further improved the detection limit to 2.0×10^{-9} M.[5] However, both the sol–gel membrane and β-CD enhanced neutral molecule based sensors suffered from the low stability of porphyrin in aqueous media and could only work within a certain pH range. To improve the stability and function of porphyrin-based sensors, amphiphilic porphyrins, such as 5,10,15,20-tetra(*p*-sulfonatophenyl)porphyrin (TPPS), were developed. A sol–gel membrane of TPPS could afford a detection limit of 7×10^{-9} M with improved stability as compared to neutral porphyrin-based mercury sensors.[6] The TPPS-based sol–gel films, however, are not suitable for long-term use since the leaching of porphyrin increased with time. To solve the problem, a *N*-trimethoxysilylpropyl-*N*′,*N*″,*N*‴-trimethylammonium chloride (TMAC)

* Corresponding author. Tel.: +65 65168049; fax: +65 67791936.
E-mail address: cheliub@nus.edu.sg (B. Liu).

0040-4039/$ - see front matter © 2008 Elsevier Ltd. All rights reserved.
doi:10.1016/j.tetlet.2008.01.138

functionalized substrate was developed to allow self-assembly of TPPS films through electrostatic interactions, which allowed the colorimetric detection of Hg^{2+} in a concentration range of 2.5×10^{-8}–5×10^{-7} M.[7] This detection strategy suffered from the interference of many other metal ions, such as Cu^{2+}, Pb^{2+} and Fe^{3+}. Recently self-assembled films of 5-(*p*-trimethylammonium trismethyleneoxyphenyl)-10,15,20-triphenylporphyrin chloride on glass were also reported, which have shown good mechanical stability with a detection limit of around 1 μM for mercury ions in aqueous solutions.[8]

The fluorescence quantum yield of most porphyrins is less than 20%, which is due to the high yield of non-irradiation decay and intersystem crossing from excited singlet state (S_1) to excited triplet state (T_1).[9] To improve the detection sensitivity of porphyrin-based optical sensors, it is of importance to develop porphyrin derivatives with high quantum yields. In addition, the degeneration of probe molecules from the solid substrate is one of the most serious problems for the long-term operation of porphyrin based solid state sensors.[4,6] It became our aim to develop high quantum yield porphyrin derivatives that could anchor the substrate with high stability. In this Letter, we report the synthesis and characterization of a new cationic porphyrin, 5,15-(*p*-(9,9-bis(6-trimethylammoniumhexyl)-fluorenylethynyl)phenyl) porphyrin tetrabromide (**1**) and its application to mercury ion detection as a self-assembled film on glass.

Dipyrromethane (**2**) and 2-bromo-9,9-bis(6-bromohexyl) fluorene (**3**) were synthesized according to previous reports.[10,11] Coupling of **3** and trimethylsilylacetylene under Sonogashira conditions afforded 2-(9,9-bis(6-bromohexyl)fluoren-7-yl)ethynyltrimethylsilane (**4**). After the removal of the trimethylsilyl group in a KOH/THF/methanol solution, 9,9-bis(6-bromohexyl)-2-ethynyl-9*H*-fluorene (**5**) was coupled with *p*-bromobenzylaldehyde to give *p*-(2-(9,9-bis(6-bromohexyl)-9*H*-fluoren-7-yl)ethynyl)-benzaldehyde (**6**) in a yield of 51%. Porphyrin **7** was prepared from **6** and **2** by a modified MacDonald condensation.[12] Continuous extraction with methanol was carried out to remove the trace chloranil. The residue was then recrystallized from chloroform and hexane to afford **7** as a purple solid. MALDI-TOF gave a clear mass spectrum of the neutral porphyrin **7**, which was consistent with the expected structure (see Fig. S1 in the Supplementary data). The ^{1}H NMR spectrum of **7** shows signals at δ 10.36, 9.44, and 9.12 ppm, representing the protons of porphyrin. The signal of the two delocalized hydrogens was found at −3.10 ppm (Scheme 1).

The cationic porphyrin **1** was synthesized through the amination of the neutral porphyrin **7** by the addition of trimethylamine to a solution of **7** in THF. Compound **1** was

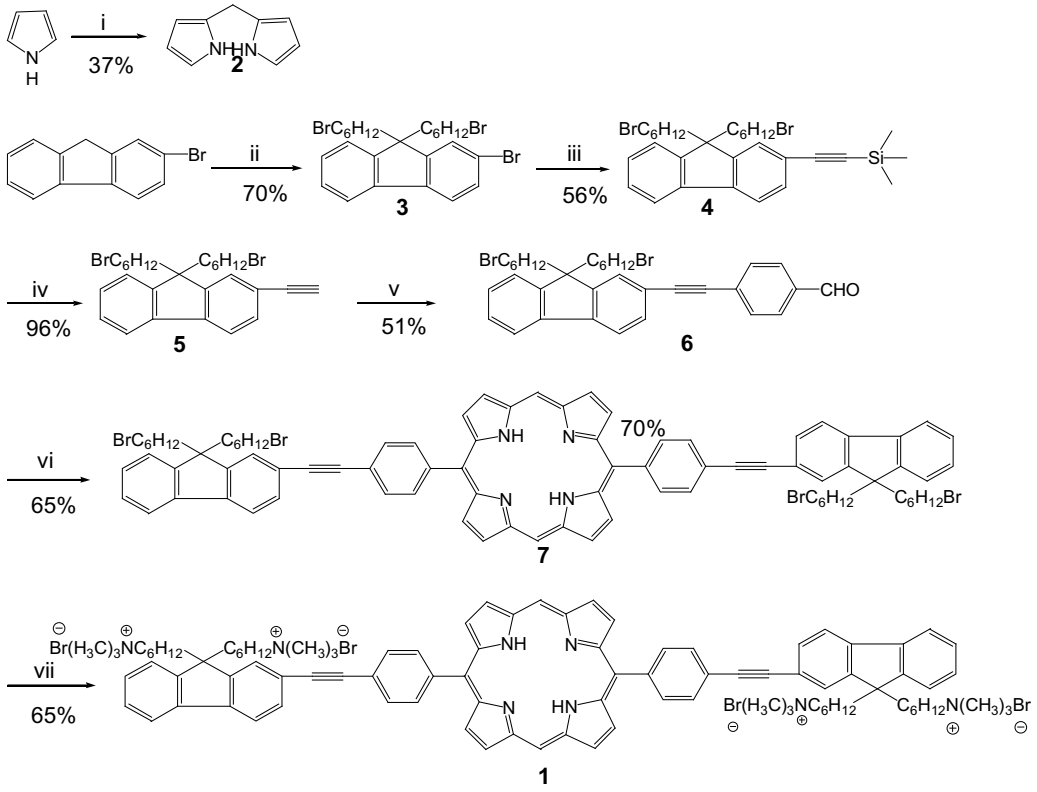

Scheme 1. Synthesis of 5,15-(*p*-(9,9-bis(6-trimethylammoniumhexyl)fluorylethynyl)phenyl) porphyrin tetrabromide (**1**). Reagents and conditions: (i) paraformaldehyde, acetic acid, MeOH, 22 h, argon; (ii) KOH, $(C_4H_9)_4NBr$, 1,6-dibromohexane, 75 °C; (iii) $(Ph_3P)_2PdCl_2$, CuI, triethylamine, trimethylsilylacetylene, 8 h, nitrogen, 70 °C; (iv) KOH, THF, MeOH, H_2O, 1 h; (v) *p*-bromobenzylaldehyde, $(Ph_3P)_2PdCl_2$, CuI, diisopropylamine, overnight, nitrogen, 70 °C; (vi) dipyrromethane **2**, CH_2Cl_2, trifluoroacetic acid, 15 h, nitrogen; chloranil, 50 °C, 1 h; (vii) trimethylamine, THF, −78 °C to room temperature, 12 h; MeOH, 20 h.

obtained as a purple solid in 65% yield. As compared to the ^{1}H NMR spectrum of **7**, the signal due to $-CH_2Br$ in the fluorene chain at δ 3.33 ppm disappeared; meanwhile a new resonance at δ 3.07 ppm corresponding to $-N(CH_3)_3$ groups appeared for the cationic porphyrin. The chemical shifts for the porphyrin, phenyl, and fluorene protons did not change obviously upon amination. However, the signal at δ −3.10 ppm disappeared for **1**, which is possibly a result of rapid proton exchange between porphyrin and deuterated methanol used for the NMR measurement. The ^{13}C NMR spectrum of **1** clearly showed seven carbons for the side chain and one corresponding to the C-9 of fluorene. Due to the limited solubility of **1** in methanol and DMSO (<5 mg/mL), only a few carbons with respect to phenyl and the porphyrin macrocycle were observed in the ^{13}C NMR spectrum.

Figure 1 shows the absorption and emission spectra of cationic porphyrin **1** in methanol and in self-assembled film state (procedure for film preparation is outlined in Supplementary data). The cationic porphyrin exhibits strong absorption at 408 nm, with four minor Q-bands at 502, 537, 577 and 631 nm, respectively, in methanol. The Soret band at 408 nm could be attributed to the π–π^* transition from the ground state S_0 to the second excited singlet state S_2. The four Q-bands are attributed to π–π^* transitions from the ground state S_0 to the different vibration levels of the first excited singlet state S_1.[13] Due to rapid vibronic relaxation from S_2 to S_1, only emission at 635 nm and 699 nm was observed and there were no emission peaks near the Soret band. The absorption and emission maxima of the self-assembled films are red-shifted by ~10 nm compared to that for **1** in methanol, which is due to the intensive intermolecular interaction in the film state.[14] The quantum yields (Φ) for **1** in methanol and **7** in THF were measured using quinine sulfate in 0.1 N H_2SO_4 as the standard (Φ = 54%). The neutral porphyrin **7** in THF has a Φ value of 15%, which is slightly higher than H_2tpp (~13% in toluene).[15] Cationic **1** has a quantum yield of ~10% in methanol, which is similar to TPPS (12% in water).[16] The effect of aggregation was investigated by adding water to a methanol solution of **1**. The fluorescence was quenched upon the addition of water, and the emission maximum was slightly red-shifted (Fig. S3 in the Supplementary data). This observation indicates that although the sp^3 carbon bridge in propeller-like fluorene would impede the regular packing of molecule **1**, the strong π–π interaction of porphyrin moieties predominates for aggregation, which leads to fluorescence quenching and emission red shift.

Figure 2 shows the effect of Hg^{2+} on the fluorescence quenching of the cationic porphyrin film self-assembled on a glass slide. With the addition of Hg^{2+}, both emission bands at 643 nm and 705 nm decreased gradually. The fluorescence quenching suggests the interaction between porphyrin and Hg^{2+}. The relationship between the fluorescence intensity and the mercury concentration is shown in Figure 3. The logarithm of the relative fluorescence value $(F - F_0)/(F_1 - F)$ is given as a linear correlation of the logarithm of Hg^{2+} concentration in the range from 10^{-10} to 10^{-6} M, which can be explained using Eq. 8 in the Supplementary data. In Figure 3, F_0 and F_1 are defined as the fluorescence intensities in the absence and presence of mercury ions, respectively. The linear quenching indicates a 1:1 (10^{-10}–10^{-6} M) complex formation as in Eq. 1 (Supplementary data), which is similar to the previous reports.[3–5] The well fitted curve could serve as a calibration standard to quantify Hg^{2+} concentration in solution. The detection limit is estimated to be approximately 10^{-10} M, where the fluorescence quenching is equal to three times the standard deviation of blank films. As compared to previously reported porphyrin-based mercury sensors,[1–7] the improved detection sensitivity for **1** indicates that at low [Hg^{2+}], the effective binding between metal ions and the porphyrin core is improved. This is due to electron delocalization along the conjugation between the fluorenylethynylphenyl moieties and the central porphyrin ring, where the relatively electron rich fluorenylethynylphenyl groups donate electrons to increase the electron density of the porphyrin macrocycle.[17]

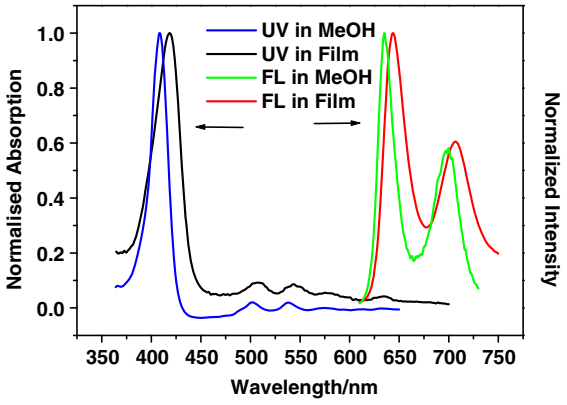

Fig. 1. UV and fluorescence (FL) spectra of **1** (1×10^{-6} M) in MeOH and in film state.

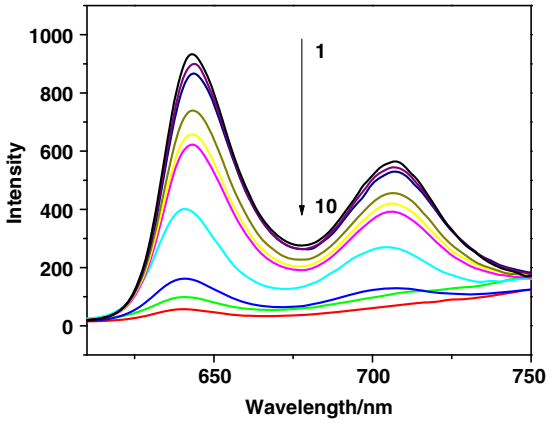

Fig. 2. Fluorescence spectra of the cationic porphyrin film after immersion in various Hg^{2+} solutions (from 1 to 10, [Hg^{2+}] = 0, 0.1, 1, 10, 60, 100 nM, 1.0, 10.0, 30.0, 100 μM).

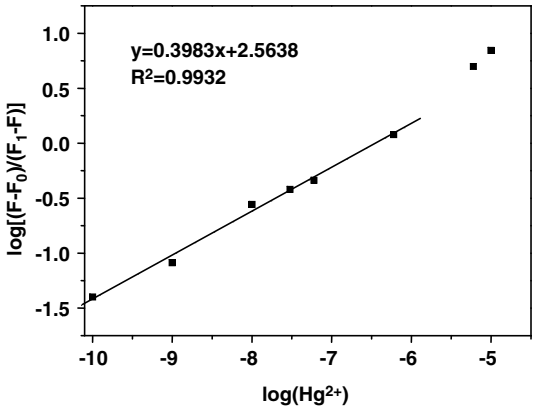

Fig. 3. log $[(F - F_0)/(F_1 - F)]$ versus log (Hg^{2+}).

By adding different amounts of potentially interfering ions (Cu^{2+}, Zn^{2+}, Pb^{2+}, Cd^{2+}, Mn^{2+}, Ni^{2+}, Co^{2+} and Ca^{2+}) to the sample solution containing 0.3 μM Hg^{2+} (~50% quenching as compared to blank), the selectivity of the porphyrin film was investigated and the results are shown in Table 1. The contaminants do not show significant interference in Hg^{2+} determination even at 1000-fold excess as compared to that of mercury. This outcome shows the high selectivity of the self-assembled porphyrin films toward Hg^{2+}.

To evaluate the stability of the porphyrin films, blank films were repeatedly immersed into pure water and dried under nitrogen before fluorescence measurement. Due to the negatively charged nature of the glass surface, static interactions bind the cationic porphyrin to the slide surface. As compared to 5-(*p*-trimethylammonium trismethyleneoxyphenyl)-10,15,20-triphenylpoyphyrin chloride, where only one positive charge was attached to the porphyrin ring, the increase in positive charge (four for **1**) greatly reduces the leaching of porphyrin into solution. For the blank films of **1**, there was no obvious change in film fluorescence intensity even after the films had been soaked and dried for 10 cycles (see Fig. S2 in the Supplementary data). Furthermore the freshly prepared porphyrin films are stable when stored under dry and dark conditions at ambient temperature. The loss of fluorescence was less than 1.5% after the films had been stored for three weeks. Both short-term and long-term measurements showed that these self-assembled films are stable, which make them suitable for the detection and determination of Hg^{2+} in aqueous solution.

Table 1
Effect of different ions on Hg^{2+} detection[a]

Entry	Concentration (M)	Relative fluorescence change value, $(F_2 - F_1)/F_1$[b] (%)
Ca^{2+} (chloride)	3×10^{-4}	−1.3
Cd^{2+} (sulfate)	3×10^{-4}	−5
Cu^{2+}(chloride)	3×10^{-5}	−7.5
Co^{2+}(chloride)	3×10^{-4}	+1.6
Mn^{2+}(sulfate)	3×10^{-4}	−3.1
Zn^{2+}(chloride)	3×10^{-4}	−4.9
Pb^{2+}(nitrate)	3×10^{-4}	−6.3
Ni^{2+}(acetate)	3×10^{-4}	−4.0
Cu^{2+}, Zn^{2+}, Pb^{2+}, Cd^{2+}, Mn^{2+}, Ni^{2+}, Co^{2+}, Ca^{2+}	3×10^{-4}[c]	−8.2

[a] Each sample solution contains a fixed Hg^{2+} concentration of 0.3 μM.
[b] F_1 and F_2 are the fluorescence intensities of porphyrin **1** in the presence of 0.3 μM Hg^{2+} without and with interfering ions, respectively.
[c] Referring to each interfering ion concentration except for the Cu^{2+} concentration which is 3×10^{-5} M.

In conclusion, we have synthesized a cationic porphyrin and developed a simple fluorometric method for the detecting and quantifying mercury ions in aqueous solution. The detection is based on the fluorescence quenching of self-assembled films on glass slides. The deposited films are highly stable in operation and storage, and are very sensitive and selective for mercury detection. A detection limit of $\sim 10^{-10}$ M was achieved, which is among the lowest for porphyrin-based Hg^{2+} detection. Under optimized conditions (e.g., temperature, pH, film thickness, etc.), further improvement is expected to yield more efficient Hg^{2+} sensors. As compared to the previously reported methods which utilize commercial porphyrins or their derivatives with slight modifications, the strategy we have developed for the synthesis of cationic porphyrins sets an example for future development of fine-tuned porphyrin-based materials for different sensor applications.

Acknowledgment

The authors are thankful to the National University of Singapore (NUS ARF R-279-000-197-112/133 and R-279-000-234-123) for financial support.

Supplementary data

Synthesis and characterization of porphyrins, operation principles, preparation of metal ions solutions, procedures to self-assemble the porphyrin films and the fluorescence of blank films. Supplementary data associated with this article can be found, in the online version, at doi:10.1016/j.tetlet.2008.01.138.

References and notes

1. Biesaga, M.; Pyrzynska, K.; Trojanowicz, M. *Talanta* **2000**, *51*, 209–224.
2. Tabata, M.; Kaneko, K. *Analyst* **1991**, *116*, 1185–1188.
3. Yeow, E. K. L.; Steer, R. P. *Phys. Chem. Chem. Phys.* **2003**, *5*, 97–105.
4. Chan, W. H.; Yang, R. H.; Wang, K. M. *Anal. Chim. Acta* **2001**, *444*, 261–269.
5. Yang, R.; Li, K.; Wang, K.; Liu, F.; Li, N.; Zhao, F. *Anal. Chim. Acta* **2002**, *469*, 285–293.
6. Plaschke, M.; Czolk, R.; Ache, H. J. *Anal. Chim. Acta* **1995**, *304*, 107–113.
7. Balaji, T.; Sasidharan, M.; Matsunaga, H. *Analyst* **2005**, *130*, 1162–1167.
8. (a) Monti, D.; Venanzi, M.; Russo, M.; Bussetti, G.; Goletti, C.; Montalti, M.; Zaccheroni, N.; Prodi, L.; Rella, R.; Manera, M. G.;

Mancini, G.; Di Natale, C.; Paolesse, R. *New J. Chem.* **2004**, *28*, 1123–1128; (b) Dolci, L. S.; Marzocchi, E.; Montalti, M.; Prodi, L.; Monti, D.; Di Natale, C.; D'Amico, A.; Paolesse, R. *Biosens. Biolectron.* **2006**, *22*, 399–404.
9. (a) Seybold, P. G.; Gouterman, M. *J. Mol. Spectrosc.* **1969**, *31*, 1–13; (b) Gradyuskho, A. T.; Tsvirko, M. P. *Opt. Spectrosc.* **1971**, *31*, 291–293; (c) Quimby, D. J.; Longo, F. R. *J. Am. Chem. Soc.* **1975**, *97*, 5111–5117.
10. Fang, Z.; Breslow, R. *Org. Lett.* **2006**, *8*, 251–254.
11. Liu, B.; Gaylord, B. S.; Wang, S.; Bazan, G. C. *J. Am. Chem. Soc.* **2003**, *125*, 6705–6714.
12. Wang, Q. M.; Bruce, D. W. *Synlett* **1995**, 1267–1268.
13. Falk, J. E. *Porphyrins and Metalloporphyrins*; Elsevier: Amsterdam, 1964.
14. Kroon, J. M.; Sudholter, E. J. R.; Schenning, A. P. H. J.; Nolte, R. J. M. *Langmuir* **1995**, *11*, 214–220.
15. Mahammed, A.; Gross, Z. *J. Inorg. Biochem.* **2002**, *88*, 305–309.
16. Knyukshto, V. N.; Solovyov, K. N.; Egorova, G. D. *Biospectroscopy* **1998**, *4*, 121–133.
17. Lebedeva, N. Sh.; Yakubov, S. P.; Vyugin, A. I.; Parfenyuk, E. V. *Thermochim. Acta* **2003**, *404*, 19–24.